# Structural analysis of mycobacterial and murine hsp60 epitopes in complex with the class I MHC molecule H-2D$^b$

Carlo Ciatto, Guido Capitani, Alain C. Tissot, Frédéric Pecorari, Andreas Plückthun, Markus G. Grütter*

*Department of Biochemistry, University of Zürich, Winterthurerstrasse 190, CH-8057 Zürich, Switzerland*

Received 5 February 2003; accepted 26 March 2003

First published online 17 April 2003

Edited by Gunnar von Heijne

**Abstract The decameric peptide SALQNAASIA from the *Mycobacterium bovis* heat shock protein (hsp) 60 is recognized by the murine T-cell receptor UZ-3-4 in complex with the murine class I major histocompatibility complex molecule H-2D$^b$. This T-cell receptor cross-reacts with the H-2D$^b$-bound non-homologous decameric peptide KDIGNIISDA from the murine hsp60, but does not recognize the nonameric mycobacterial peptide SALQNAASI. Cross-recognition of the KDIGNIISDA/H-2D$^b$ complex induces autoimmune pathology in immunodeficient mice. We solved the X-ray crystal structure of the SALQNAASIA/H-2D$^b$ complex at 3.0 Å resolution, and we modelled the KDIGNIISDA and SALQNAASI peptides in the H-2D$^b$ binding site. The structural analysis of the H-2D$^b$-bound hsp60 epitopes offers insight into T-cell receptor cross-reactivity.**


*Key words:* X-ray crystal structure; Major histocompatibility complex; T-cell receptor; Cross-reactivity

## 1. Introduction

Heat shock proteins (hsps) are phylogenetically highly conserved. Within the hsp60 family, the sequence identity between proteins from organisms as diverse as mammals and mycobacteria is approximately 50%, and the similarity is 70%. *Mycobacterium tuberculosis* is the causative agent of tuberculosis (TB), while an attenuated strain of *Mycobacterium bovis*, Bacille Calmette-Guérin (BCG), is used as a vaccine against TB. Recently, naked DNA encoding the hsp60 from *Mycobacterium leprae* (95% identical to the *M. tuberculosis* hsp60) was tested as a subunit vaccine in mice [1], the animal model of choice for TB. The naked DNA vaccine provided protection comparable to BCG, and was also successfully used as a therapeutic agent for the treatment of infected mice [2]. In both cases, the positive effects were accompanied by activation of antigen-specific, CD8$^+$ T-cell-mediated cellular immunity. Cellular cytotoxicity has been recognized as an important aspect of the immune response against TB [3,4].

The high similarity among hsp60s suggests the possibility of immunological cross-reactivity between hsp60s of self and pathogenic origins, with important implications for vaccine safety. In vitro studies showed that major histocompatibility complex (MHC) class I-restricted CD8$^+$ T-cells raised against mycobacterial hsp60 cross-react with stressed murine host cells [5]. The *M. bovis* epitope, which is recognized by the cross-reactive T-cell clone UZ-3-4 when bound to the class I MHC molecule H-2D$^b$, was identified as the decameric peptide SALQNAASIA (hsp60$_{499-508}$) [6]. This peptide does not conform to the optimal H-2D$^b$ binding motif [7], which has Asn in P5 and a bulky hydrophobic residue in PΩ (C-terminal amino acid). The optimal peptide for binding to H-2D$^b$, the nonameric peptide SALQNAASI (hsp$_{499-507}$), does bind to H-2D$^b$, but is not recognized by the T-cell receptor (TCR) UZ-3-4 [6]. The murine epitope recognized by UZ-3-4 also came from the hsp60; however, the cross-reacting antigen did not correspond to the homologous murine sequence, but rather to the peptide KDIGNIISD(A) (hsp60$_{162-170/171}$) [8], which shows low identity with the mycobacterial epitope.

Both immunization with mycobacterial hsp60 [4,8] and vaccination with BCG [4] stimulated CD8$^+$ T-cell clones specific for the mycobacterial peptide hsp60$_{499-508}$, and these T-cells cross-reacted with the murine hsp60$_{162-170/171}$. The use of mycobacterial hsp60 for vaccine design thus carries the danger of an autoimmune response; adoptive transfer of the UZ-3-4 T-cell clone in immunodeficient mice indeed induced autoimmune pathology [9].

We have previously analyzed the TCR expressed by the T-cell clone UZ-3-4, and its interaction with the mycobacterial peptide hsp60$_{499-508}$ SALQNAASIA (termed ASIA for short) in complex with H-2D$^b$ [10]. In the present study, we extend our biophysical characterization of the molecules involved in the protective immune response and the autoimmune reaction described above. We have solved the crystal structure, determined at 3.0 Å resolution, of the ASIA/H-2D$^b$ complex, and we have modelled both the mycobacterial peptide hsp60$_{499-507}$ SALQNAASI (termed ASI for short), and the murine peptide hsp60$_{162-171}$ KDIGNIISDA (termed ISDA for short), in the H-2D$^b$ binding site. A comparison of the three peptide/H-2D$^b$ complexes offers an insight into the cross-reactivity of the TCR UZ-3-4.

*Corresponding author. Fax: (41)-1-6356834.
*E-mail address:* gruetter@bioc.unizh.ch (M.G. Grütter).

*Abbreviations:* MHC, major histocompatibility complex; pMHC, peptide/MHC complex; SAS, solvent-accessible surface; TCR, T-cell receptor

0014-5793/03/$22.00 
doi:10.1016/S0014-5793(03)00325-9

## 2. Materials and methods

### 2.1. Protein expression and purification

The SALQNAASIA/H-2D$^b$ complex was prepared as previously reported [10].

### 2.2. Crystallization

Crystals were grown by the hanging drop vapor diffusion method, by mixing 2 μl of protein solution with 2 μl of reservoir solution at 4°C. The protein solution (10 mg/ml) contained 150 mM NaCl and 20 mM Tris, pH 8.0. The reservoir solution contained 2.0 M ammonium sulfate, 15% v/v glycerol, and 0.1 M Tris, pH 8.0.

### 2.3. Data collection and processing

A full dataset was collected to a maximum resolution of 3.0 Å, from a crystal flash-frozen in a stream of liquid $N_2$ at 100 K. The data were collected at the Swiss–Norwegian Beam Line, Station BM1A, at the ESRF, Grenoble, France.

The data were processed and scaled with the HKL package [11] (Denzo and Scalepack). The crystal belongs to the space group C2. Data statistics are presented in Table 1.

### 2.4. Structure solution and refinement

The structure was solved by molecular replacement with AMoRe [12], using the Flu/H-2D$^b$ complex [13] (PDB code: 1HOC) as a search model, after removal of the peptide. Four H-2D$^b$ molecules were found in the asymmetric unit.

Cycles of structure refinement in CNS [14] were alternated with manual rebuilding of the model in O [15]. The peptide was initially added as a poly-alanine model, and the appropriate side chains were introduced at later stages. Strong non-crystallographic symmetry restraints (300 kcal/mol/Å$^2$) were applied at the beginning of the refinement, and were partially released (100 kcal/mol/Å$^2$) at the end. Grouped *B* factor refinement was performed, refining two *B* values per residue (main chain and side chain atoms). The final $R_{work}$ and $R_{free}$ were 24.6% and 30.7%. A summary of the crystallographic statistics is shown in Table 1. The atomic coordinates and structure factors have been deposited in the Protein Data Bank (PDB code: 1N3N)

### 2.5. Molecular modeling

The molecular models of the ISDA/H-2D$^b$ and ASI/H-2D$^b$ complexes are based on the crystal structure of ASIA/H-2D$^b$ (this study) and Flu/H-2D$^b$ [13], respectively. The peptide side chains were manually mutated in O; rotamer selection was based on potential hydrogen bonds and steric complementarity with the H-2D$^b$ binding site. Afterwards, 200 steps of conjugate gradient minimization were performed in CNS.

## 3. Results

### 3.1. Crystal structure of the ASIA/H-2D$^b$ complex

In the final model, four peptide/H-2D$^b$ complexes are present in the asymmetric unit (MolA, MolB, MolC, and MolD). MolA and MolB have the same orientation in the

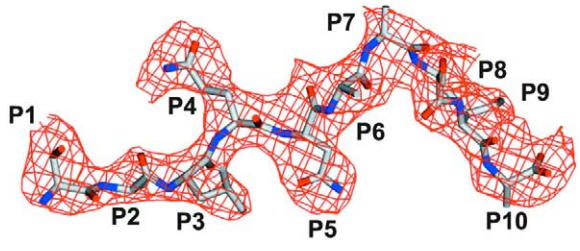


Fig. 1. Electron density map of the H-2D$^b$-bound ASIA peptide. The peptide is oriented above the floor of the binding site, and is viewed from the α2-helix side of the MHC heavy chain. The α1-helix is behind the peptide. The $F_o-F_c$ simulated annealing (2000 K) omit map is contoured at the 2.5 σ level. Picture made in SETOR [35].

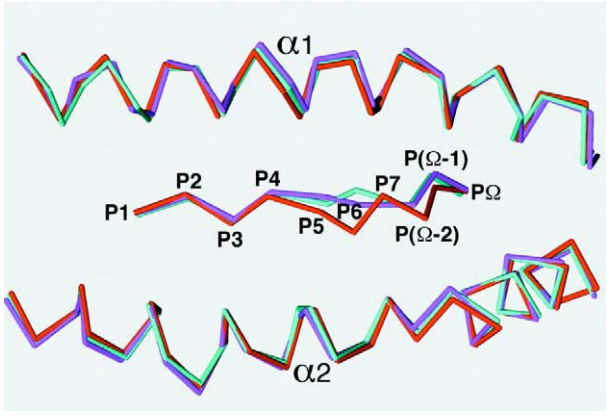


Fig. 2. Top view of the H-2D$^b$ binding site, showing the $C_\alpha$ trace of the ASIA peptide (red) superimposed on the influenza virus (purple) and Sendai virus (cyan) peptides. The superposition is based on the $C_\alpha$ atoms of the α1- and α2-helices, which are also shown. Picture made with SETOR [35].

Table 1
Crystallographic statistics

| | |
|---|---|
| Space group | C2 |
| Cell parameters | |
| *a* (Å) | 129.28 |
| *b* (Å) | 123.00 |
| *c* (Å) | 150.83 |
| *α* (°) | 90 |
| *β* (°) | 90.01 |
| *γ* (°) | 90 |
| Molecules per asymmetric unit | 4 |
| Data collection | |
| Resolution limit (Å) | 3.00 |
| Outermost shell (Å) | 3.11–3.00 |
| Unique reflections[a] | 47 412 (4725) |
| Redundancy[a] | 3.8 (3.8) |
| Completeness[a] (%) | 99.9 (100.0) |
| Average $I/\sigma$[a] | 13.6 (4.5) |
| $R_{merge}$ [a,b] (%) | 9.3 (40.0) |
| Refinement | |
| $R_{work}$ [c] (%) | 24.6 |
| $R_{free}$ [d] (%) | 30.7 |
| Number of water molecules | 189 |
| Rmsd bonds (Å) | 0.013 |
| Rmsd angles (°) | 1.54 |
| Average B values (Å$^2$) | |
| All protein atoms | 53.6 |
| MHC | 54.0[e] |
| Peptide | 36.9[e] |
| Waters | 26.1 |
| Ramachandran plot regions[f] | |
| Most favored regions (%) | 81.1 |
| Additional allowed regions (%) | 17.7 |
| Generously allowed regions (%) | 1.2 |
| Disallowed regions (%) | 0.0 |

[a]Numbers in parentheses refer to the outermost resolution shell.
[b]$R_{merge} = \sum_{hkl}\sum_j |I_{j,hkl} - \langle I_{hkl}\rangle| / \sum_{hkl}\sum_j I_{j,hkl}$, where $\langle I_{hkl}\rangle$ is the average of the intensity $I_{j,hkl}$ over $j = 1, ..., N$ observations of symmetry-equivalent reflections *hkl*.
[c]$R_{work} = (\sum_{hkl} ||F_o| - |F_c||) / \sum_{hkl} |F_o|$, where $|F_o|$ and $|F_c|$ are the observed and calculated structure factor amplitudes, respectively.
[d]$R_{free}$ is the same as $R_{work}$ but is calculated using 3% of the reflections that were excluded from the refinement.
[e]This value refers to all four molecules in the asymmetric unit.
[f]Calculated with PROCHECK [37].

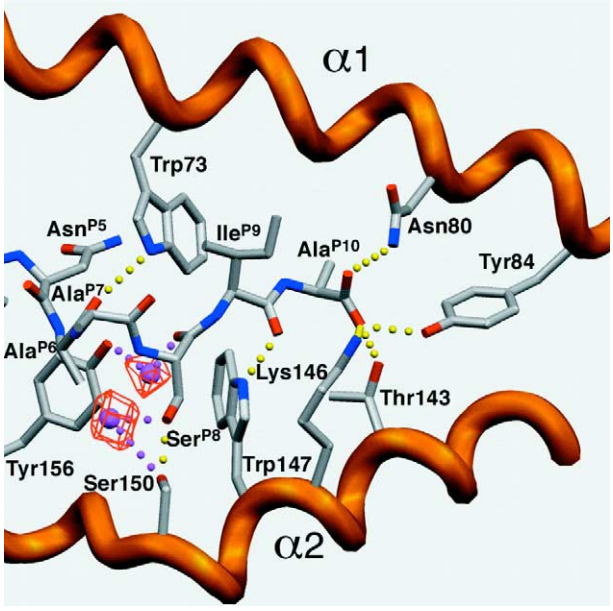


Fig. 3. Crucial interactions between the C-terminal half of the ASIA peptide and the H-2D$^b$ binding groove. The backbones of the α1- and α2-helices are shown as orange ribbons. Hydrogen bonds between peptide and MHC are shown as yellow dots. Two water molecules (purple), mediating further hydrogen bonds (purple), are shown in an $F_o-F_c$ omit map, contoured at the 3.5 σ level. Picture made in SETOR [35].

asymmetric unit, and are related by simple translation; the same relationship applies to MolC and MolD. The average root mean square deviation for the $C_\alpha$ of the bound peptides is 0.17 Å; our analysis will be restricted to the peptide bound to MolA.

Peptide binding to a given class I MHC molecule requires the presence of 'anchor residues', which complement the physicochemical characteristics of the specificity pockets [16] of the MHC molecule's binding site. In the case of the murine H-2D$^b$, the peptide binding motif [7] includes Asn in P5 and an Ile/Leu/Met at the C-terminal position (PΩ), which generally corresponds to position 9. However, exceptions are known regarding both anchor residues [17] and peptide length [18]. The decameric peptide ASIA, shown in Fig. 1, presents a double exception, being longer and possessing a non-standard

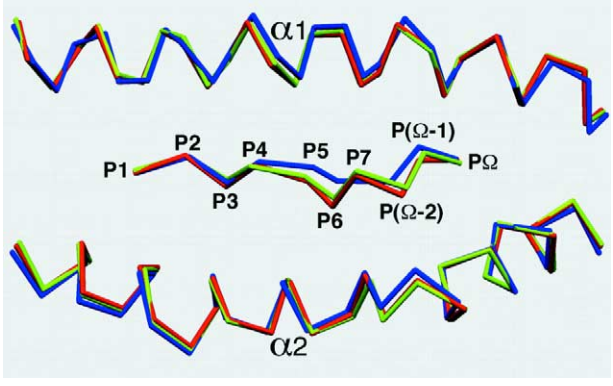


Fig. 4. Top view of the H-2D$^b$ binding site, showing the $C_\alpha$ trace of the ASIA peptide (red) superimposed on the modeled ISDA (green) and ASI (blue) peptides. The superposition is based on the $C_\alpha$ atoms of the α1- and α2-helices, which are also shown. Picture made with SETOR [35].

PΩ anchor residue (Ala$^{P10}$). For comparison, Fig. 2 shows a superposition in the MHC binding groove of ASIA and two nonameric peptides of known crystal structure. The two peptides are from Sendai virus (FAPGNYPAL) [19], and from influenza virus (Flu, ASNENMETM) [13]. In our crystal structure, the side chain of Ala$^{P10}$ leaves an 80 Å$^3$ void in the F pocket (volume calculated with Voidoo [20], using a 1.4 Å radius rolling probe). In other crystal structures of peptide/H-2D$^b$ complexes [13,17,18,21] the large, hydrophobic F pocket is filled up by PΩ residues that have bulky, hydrophobic side chains. Nevertheless, the position of the Ala$^{P10}$ $C_\alpha$ is unchanged (Fig. 2), and the C-terminal carboxylate forms a set of conserved hydrogen bonds with H-2D$^b$ side chains (Fig. 3). H-2D$^b$-bound peptides form a pronounced bulge in their C-terminal portion [13,17,18,21], between the anchor positions P5 and PΩ, due to the presence of a hydrophobic ridge (formed by Trp73, Trp147, and Tyr156) that lies across the binding site; such a bulge is more pronounced in longer peptides [18], where more residues are interposed between the anchors. The decameric ASIA peptide rises above the floor of the binding site and kinks (Fig. 2) between Ala$^{P6}$ and Ser$^{P8}$. Consequently, Ala$^{P7}$ is completely solvent-exposed, and contributes 111 Å$^2$ to the total of 264 Å$^2$ solvent-accessible surface (SAS) of the peptide (areas calculated with Areaimol [22], using a 1.7 Å radius probe). The only other residue that contributes significantly to the SAS is Gln$^{P4}$ (86 Å$^2$). The carbonyl oxygen of Ala$^{P6}$ is hydrogen-bonded to Trp73 $N_{\varepsilon 1}$, and the Ser$^{P8}$ carbonyl oxygen is hydrogen-bonded, via a water molecule, to Tyr156 of the heavy chain (Fig. 3): this pair of hydrogen bonds was shown to drive the position of the

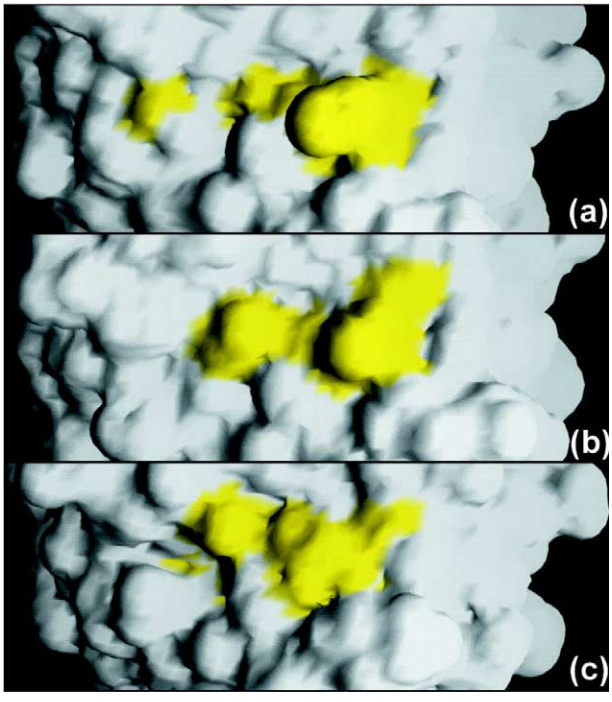


Fig. 5. Surface representation of the hsp60-derived peptide/H-2D$^b$ complexes, showing the variation in solvent accessibility of the antigenic peptides. The binding sites are viewed from the top; the MHC atoms are mapped onto the surface in white, and the peptides in yellow. The C-terminal ends of the peptides are on the right. a: The modeled ISDA peptide; b: the ASIA peptide; c: the modeled ASI peptide. Picture made with GRASP [36].

P6 $C_\alpha$ towards the α2-helix [18,21]. Another crucial interaction for determining the peculiar conformation of ASIA is between $Ser^{P8}$ and Ser150, which is located on the α2-helix; the two residues form a hydrogen bond (Fig. 3), and an ordered water molecule cross-links their side chains. The net result of this hydrogen bond network is an overall shift of the peptide backbone towards the α2-helix of the MHC molecule, when compared to other H-2D$^b$-bound peptides (Fig. 2 and Fig. 2a in [18]). This shift occurs between P5 and P10; only the extra residue, $Ala^{P7}$, is positioned towards the center of the binding groove.

### 3.2. Modeling of ASI and ISDA in the H-2D$^b$ binding site

The nonameric mycobacterial peptide ASI and the decameric murine peptide ISDA were modeled in the H-2D$^b$ binding site based on the nonameric Flu structure [13] and the decameric ASIA structure, respectively. The choice of the Flu complex [13] is justified by its bound peptide having an 'intermediate' conformation among H-2D$^b$-bound nonameric peptides [18], with the backbone positioned close to the center of the binding cleft. The ASIA complex was chosen since it is the only known H-2D$^b$ structure that contains a decameric peptide. Fig. 4 shows that assigning the role of C-terminal anchor residue to $Ile^{P9}$ of ASI forces the peptide backbone in an extended conformation, as seen in other nonameric peptides (Fig. 2). This drastically decreases the peptide's SAS to 204 Å$^2$, with a dominant contribution from $Gln^{P4}$ (72 Å$^2$) and $Ala^{P6}$ (54 Å$^2$). Conversely, the decameric peptide ISDA, which binds to H-2D$^b$ using $Ala^{P10}$ as C-terminal anchor residue, is predicted to retain a conformation which is comparable to ASIA (Fig. 4). Despite its bulkier side chain, $Ile^{P6}$ can be accommodated on a hydrophobic shelf that forms the D pocket [16], with a small deviation of the $C_\alpha$ position towards the center of the binding site (Fig. 4). The position of $Ser^{P8}$ is conserved, as well as its interaction with the α2-helix. The backbone kink at position P7 is preserved, and $Ile^{P7}$ contributes 191 Å$^2$ to the peptide's SAS (313 Å$^2$); the P4 residue (Gly) now has a very small SAS (23 Å$^2$).

## 4. Discussion

In the ASIA/H-2D$^b$ crystal structure, the anchor residue $Ala^{P10}$ only partially fills the F pocket, leaving an 80 Å$^3$ cavity in the binding groove. The presence of cavities at the peptide/MHC interface has been associated with decreased thermal stability of the peptide/MHC complex (pMHC) [23]. The substitution of a pocket-filling PΩ anchor residue, such as Leu [18,19], with Ala should be accompanied by a free energy cost [24]. This can be approximated as a constant term (~2 kcal/mol), which is equivalent to the transfer free energy from water to organic solvent of Leu relative to Ala, and a variable term (24–33 cal/mol/Å$^3$), which is proportional to the cavity volume [24]. In the present case, the estimated free energy cost of using Ala instead of Leu as the PΩ anchor is between 3.9 and 4.6 kcal/mol. In contrast, a similar substitution in the influenza virus matrix peptide bound to the human HLA-A2 did not change the thermal stability of the complex [25]. The energetic cost of this substitution is therefore undetermined for H-2D$^b$, and must be measured experimentally. Thus the question remains open whether the preference shown by F pockets for bulky hydrophobic residues, such as Leu rather than Ala, is intrinsic to H-2D$^b$ (and HLA-A2 as well), or stems merely from the specificity of the proteasome [26], which generates the C-terminus of antigenic peptides.

The murine T-cell clone UZ-3-4, obtained from mice immunized with mycobacterial hsp60, was shown to be specific for the H-2D$^b$-bound *M. bovis* hsp60 epitope ASIA [6], and to cross-react with the murine hsp60 epitope ISDA [8]. In contrast, the *M. bovis* hsp60 peptide ASI is not recognized [6]. The crystal structure presented here shows that the decameric peptide ASIA bound to H-2D$^b$ assumes a peculiar conformation (Fig. 2 and [18]), which is distinct from other H-2D$^b$-bound peptides. The shift of the C-terminal part of the peptide from the center of the binding groove towards the α2-helix and the kink observed in P7 are determined by the length of the peptide (10 residues), the use of Ala as the PΩ anchor residue, and the presence of Ser in position PΩ−2 (Fig. 3). These features are present in ISDA, but not in ASI. Despite the low sequence identity (3/10) and similarity (6/10), the ISDA/H-2D$^b$ model shows that ISDA can retain the same backbone conformation as ASIA (Fig. 4). TCR recognition is generally thought to use flexible binding surfaces [27], and a two-step mechanism where peptide contact follows docking onto the MHC [28]. Both features favor cross-reactivity towards MHC-bound peptides that retain a sufficient level of structural similarity. The increased SAS of ISDA (Fig. 5a) in comparison with ASIA (Fig. 5b) is mostly due to the Ala to Ile mutation in P7. The $K_D$ describing the UZ-3-4/ASIA/H-2D$^b$ interaction is ~100 μM [10], which puts it in the low affinity range for TCR recognition, and hints at a poor surface complementarity at the TCR/pMHC interface [29]. The bulky $Ile^{P7}$ in ISDA (Fig. 5a) could promote better interaction with UZ-3-4. A similar effect was observed for the A6 TCR interacting with alkyl substitutes of a Tax peptide mutant bound to HLA-A2 [29], where better packing at the TCR/pMHC interface lead to higher affinity. Importantly, a $K_D$ lower than 100 μM, reflecting higher affinity for the murine self-peptide ISDA bound to H-2D$^b$, would not exceed the affinity threshold ($K_D \approx 10$ μM [30]) for positive thymocyte selection, and would thus allow the conservation of UZ-3-4 in the murine TCR repertoire.

Modeling shows that ASI in complex with H-2D$^b$ cannot assume the peculiar backbone conformation shared by ASIA and ISDA (Fig. 4). Furthermore, crystal structures of TCR/pMHC complexes show that antigenic peptides contribute, on average, 250 Å$^2$ to the TCR/pMHC interface [31], and only in one case less than 200 Å$^2$. The total SAS of ASI (Fig. 5c) in complex with H-2D$^b$ is an inconspicuous 204 Å$^2$, and only 100 Å$^2$ for its C-terminal portion; these simple facts can explain the lack of recognition by UZ-3-4.

The high immunogenicity of microbial heat shock proteins (reviewed in [32]) makes them attractive candidates for subunit vaccine development, and hsp60 has been used with success for a naked DNA vaccine against TB [1,2] in mice. At the same time, the high similarity between hsp60 in mycobacteria and mammals raises concerns about the possibility of cross-reaction and an induced autoimmune response [32]. Indeed, TCR cross-recognition of the mycobacterial and murine hsp60 was observed [8], as well as hsp60-linked autoimmune pathology [9]. However, the present study suggests that the observed cross-recognition of self and non-self hsp60 epitopes by the TCR UZ-3-4 strictly depends on the restricting class I MHC molecule, H-2D$^b$. It is noteworthy that most of the DNA vaccine experiments [1,2] were performed in BALB/c mice

(H-2$^d$ haplotype), which do not express H-2D$^b$. BALB/c mice express H-2L$^d$, which is similar in sequence [33] to H-2D$^b$, and in structure [34], since also its binding groove possesses the hydrophobic ridge composed of Trp73, Trp147, and Tyr156. Nevertheless, H-2L$^d$ prefers Pro as the P2 anchor residue, and will not bind ASIA or ISDA. Therefore, the absence of adverse effects in inbred BALB/c may be attributed to their specific genetic make-up.

In conclusion, our analysis shows that cross-reactivity between homologous self and non-self antigens can be due to subtle structural factors which cannot be revealed by sequence similarity, and that the genetic background of the animal models is of importance. Incorporation of this kind of structural information can also help in the rational analysis of new vaccines.

*Acknowledgements:* We thank Dr. K. Diederichs for advice in data processing, and M. Tschopp for technical assistance. Experimental assistance from the staff of the Swiss–Norwegian Beam Lines at ESRF (Grenoble, France) is gratefully acknowledged. This work was supported by the Swiss National Science Foundation and by a grant to M.G.G. from the Baugarten Foundation, Zürich, Switzerland.

## References

[1] Tascon, R.E., Colston, M.J., Ragno, S., Stavropoulos, E., Gregory, D. and Lowrie, D.B. (1996) Nat. Med. 2, 888–892.
[2] Lowrie, D.B., Tascon, R.E., Bonato, V.L., Lima, V.M., Faccioli, L.H., Stavropoulos, E., Colston, M.J., Hewinson, R.G., Moelling, K. and Silva, C.L. (1999) Nature 400, 269–271.
[3] Orme, I.M. (1993) Trends Microbiol. 1, 77–78.
[4] Zügel, U. and Kaufmann, S.H.E. (1997) Infect. Immun. 65, 3947–3950.
[5] Koga, T., Wand-Württenberger, A., DeBruyn, J., Munk, M.E., Schoel, B. and Kaufmann, S.H.E. (1989) Science 245, 1112–1115.
[6] Schoel, B., Zügel, U., Ruppert, T. and Kaufmann, S.H.E. (1994) Eur. J. Immunol. 24, 3161–3169.
[7] Falk, K., Rötzschke, O., Stevanovic, S., Jung, G. and Rammensee, H.G. (1991) Nature 351, 290–296.
[8] Zügel, U., Schoel, B., Yamamoto, S., Hengel, H., Morein, B. and Kaufmann, S.H.E. (1995) Eur. J. Immunol. 25, 451–458.
[9] Steinhoff, U., Brinkmann, V., Klemm, U., Aichele, P., Seiler, P., Brandt, U., Bland, P.W., Prinz, I., Zügel, U. and Kaufmann, S.H.E. (1999) Immunity 11, 349–358.
[10] Pecorari, F., Tissot, A.C. and Plückthun, A. (1999) J. Mol. Biol. 285, 1831–1843.
[11] Otwinowski, Z. and Minor, W. (1997) Methods Enzymol. 276, 307–326.
[12] Navaza, J. (1994) Acta Crystallogr. A 50, 157–163.
[13] Young, A.C., Zhang, W., Sacchettini, J.C. and Nathenson, S.G. (1994) Cell 76, 39–50.
[14] Brünger, A.T., Adams, P.D., Clore, G.M., DeLano, W.L., Gros, P., Grosse-Kunstleve, R.W., Jiang, J.S., Kuszewski, J., Nilges, M., Pannu, N.S., Read, R.J., Rice, L.M., Simonson, T. and Warren, G.L. (1998) Acta Crystallogr. D 54, 905–921.
[15] Jones, T.A., Zou, J.Y., Cowen, S.W. and Kjeldgaard, M. (1991) Acta Crystallogr. A 47, 110–119.
[16] Saper, M.A., Bjorkman, P.J. and Wiley, D.C. (1991) J. Mol. Biol. 219, 277–319.
[17] Ostrov, D.A., Roden, M.M., Shi, W., Palmieri, E., Christianson, G.J., Mendoza, L., Villaflor, G., Tilley, D., Shastri, N., Grey, H., Almo, S.C., Roopenian, D. and Nathenson, S.G. (2002) J. Immunol. 168, 283–289.
[18] Ciatto, C., Tissot, A.C., Tschopp, M., Capitani, G., Pecorari, F., Plückthun, A. and Grütter, M.G. (2001) J. Mol. Biol. 312, 1059–1071.
[19] Glithero, A., Tormo, J., Haurum, J.S., Arsequell, G., Valencia, G., Edwards, J., Springer, S., Townsend, A., Pao, Y.L., Wormald, M., Dwek, R.A., Jones, E.Y. and Elliott, T. (1999) Immunity 10, 63–74.
[20] Kleywegt, G.J. and Jones, T.A. (1994) Acta Crystallogr. D 50, 178–185.
[21] Tissot, A.C., Ciatto, C., Mittl, P.R., Grütter, M.G. and Plückthun, A. (2000) J. Mol. Biol. 302, 873–885.
[22] Collaborative Computational Project, Number 4 (1994) Acta Crystallogr. D 50, 760–763.
[23] Apostolopoulos, V., Yu, M., Corper, A.L., Teyton, L., Pietersz, G.A., McKenzie, I.F. and Wilson, I.A. (2002) J. Mol. Biol. 318, 1293–1305.
[24] Eriksson, A.E., Baase, W.A., Zhang, X.J., Heinz, D.W., Blaber, M., Baldwin, E.P. and Matthews, B.W. (1992) Science 255, 178–183.
[25] Bouvier, M. and Wiley, D.C. (1994) Science 265, 398–402.
[26] Toes, R.E., Nussbaum, A.K., Degermann, S., Schirle, M., Emmerich, N.P., Kraft, M., Laplace, C., Zwinderman, A., Dick, T.P., Müller, J., Schönfisch, B., Schmid, C., Fehling, H.J., Stevanovic, S., Rammensee, H.G. and Schild, H. (2001) J. Exp. Med. 194, 1–12.
[27] Willcox, B.E., Gao, G.F., Wyer, J.R., Ladbury, J.E., Bell, J.I., Jakobsen, B.K. and van der Merwe, P.A. (1999) Immunity 10, 357–365.
[28] Wu, L.C., Tuot, D.S., Lyons, D.S., Garcia, K.C. and Davis, M.M. (2002) Nature 418, 552–556.
[29] Baker, B.M., Gagnon, S.J., Biddison, W.E. and Wiley, D.C. (2000) Immunity 13, 475–484.
[30] Alam, S.M., Travers, P.J., Wung, J.L., Nasholds, W., Redpath, S., Jameson, S.C. and Gascoigne, N.R. (1996) Nature 381, 616–620.
[31] Rudolph, M.G. and Wilson, I.A. (2002) Curr. Opin. Immunol. 14, 52–65.
[32] Zügel, U. and Kaufmann, S.H.E. (1999) Clin. Microbiol. Rev. 12, 19–39.
[33] Rubocki, R.J., Lee, D.R., Lie, W.R., Myers, N.B. and Hansen, T.H. (1990) J. Exp. Med. 171, 2043–2061.
[34] Balendiran, G.K., Solheim, J.C., Young, A.C., Hansen, T.H., Nathenson, S.G. and Sacchettini, J.C. (1997) Proc. Natl. Acad. Sci. USA 94, 6880–6885.
[35] Evans, S.V. (1993) J. Mol. Graph. 11, 134–138.
[36] Nicholls, A., Sharp, K.A. and Honig, B. (1991) Proteins 11, 281–296.
[37] Laskowski, R.A., MacArthur, M.W., Moss, D.S. and Thornton, J.M. (1993) J. Appl. Crystallogr. 26, 283–291.